THE JOURNAL OF PHYSICAL CHEMISTRY B

ARTICLE

pubs.acs.org/JPCB

Long-Term-Stable Ether−Lipid vs Conventional Ester−Lipid Bicelles in Oriented Solid-State NMR: Altered Structural Information in Studies of Antimicrobial Peptides

Kresten Bertelsen,[†] Brian Vad,[‡] Erik H. Nielsen,[†] Sara K. Hansen,[†] Troels Skrydstrup,[†] Daniel E. Otzen,[‡] Thomas Vosegaard,[*,†] and Niels Chr. Nielsen[*,†]

[†]Center for Insoluble Protein Structures (inSPIN), Interdisciplinary Nanoscience Center (iNANO) and Department of Chemistry, Aarhus University, DK-8000 Aarhus C, Denmark

[‡]Centre for Insoluble Protein Structures (inSPIN), Interdisciplinary Nanoscience Center (iNANO) and Department of Molecular Biology, Aarhus University, DK-8000 Aarhus C, Denmark

ABSTRACT: Recently, ether lipids have been introduced as long-term stable alternatives to the more natural, albeit easier degradable, ester lipids in the preparation of oriented lipid bilayers and bicelles for oriented-sample solid-state NMR spectroscopy. Here we report that ether lipids such as the frequently used 14-O-PC (1,2-di-*O*-tetradecyl-*sn*-glycero-3-phosphocholine) may induce significant changes in the structure and dynamics, including altered interaction between peptides and lipids relative to what is observed with the more conventionally used DMPC (1,2-dimyristoyl-*sn*-glycero-3-phosphocholine) bilayers. Such effects are demonstrated for the antimicrobial peptide novicidin, for which 2D separate-local-field NMR and circular dichroism experiments reveal significant structural/conformational differences for the peptide in the two different lipid systems. Likewise, we observe altered secondary structure and different temperature-dependent membrane anchoring for the antimicrobial peptide alamethicin depending on whether the peptide is reconstituted into ester or ether lipids. Such observations are not particularly surprising considering the significant difference of the lipids in the phosphorus headgroup and they may provide important new insight into the delicate peptide−membrane interactions in the systems studied. In contrast, these observations reinforce the need to carefully consider potential structural changes in addition to long-term stability prior to the selection of membrane environment of membrane proteins in the analysis of their structure and dynamics. In more general terms, the results underscore the necessity in structural biology to address both the protein and its environments in studies relating structure to function.

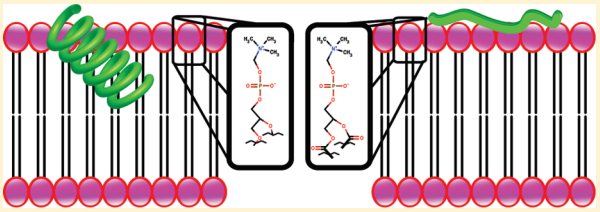

1. INTRODUCTION

Oriented-sample solid-state NMR has attracted much attention as a method to study structure, conformation, and dynamics of membrane proteins and peptides embedded in hydrated lipid bilayers.[1−6] The method relies on measurement of "single-crystal"-like sharp resonances providing information about anisotropic (i.e., orientation-dependent) as well as isotropic nuclear spin interactions. The success of the method highly depends on the ability to align the sample uniformly relative to the external magnetic field. Consequently, substantial effort has been devoted to establishing lipid systems that, at the same time, as closely as possible mimic the in situ membrane of living cells, can be properly macroscopically or magnetically aligned, are long-term stable, and have parameters such as lipid composition, hydration, temperature, and pH to be controlled by the investigator. Model systems encompassing mechanically oriented bilayers incorporated between stacks of glass slides[7−9] as well as magnetically oriented bicelles[10−12] have been proposed for such studies. The former system enables a high degree of flexibility with respect to lipid composition, hydration, and temperature. For this system, however, disadvantages include difficulties in maintaining the sample hydrated and oriented during many hours/days of experiments with strong rf irradiation as well as imposing the need for nontraditional/suboptimal rf coil designs to obtain a good rf filling factor. The bicelles, composed of long-chain and a short-chain lipid components forming the planar and rim parts of disk-shaped particles, respectively, possess sufficient magnetic susceptibility to spontaneously align the bicelles in a magnetic field. This provides a means for easy sample preparation and good alignment. However, this system is much less flexible with respect to designing particles with the right size, orientation properties, and lipid composition. Furthermore, bicelles tend to hydrolyze and thereby lose their alignment over time,[13] in particular at nonneutral pH.

To establish bicelles and oriented planar membranes with improved long-term stability, it has been proposed to replace the most typical ester lipids with ether variants.[13,14] These lipids are much more resistant toward hydrolyzation and are therefore suggested to be better suited as a host for expensive isotope-labeled

Received: November 14, 2010
Revised: January 7, 2011
Published: February 10, 2011

ACS Publications © 2011 American Chemical Society

peptides/proteins requiring many different experiments and long measuring times. It is intuitively clear, however, that fundamental changes in the lipid headgroup may cause altered membrane properties[15] and change the lipid−peptide/protein interactions.[16,17] Exactly this feature makes the natural distribution of ester and ether lipids very distinct with the latter being much less frequently distributed, and primarily found in the membranes of microorganisms subject to extreme conditions such as *Archaea* bacteria, and they are even proposed to have antioxidant and cytotoxic properties.[18] With origin in the natural diversity of the lipids, this paper demonstrates that the molecular conformation and secondary structure of membrane-embedded peptides/proteins may be severely altered in ether bicelles as compared to ester bicelles. Accordingly, we recommend that care be taken when using ether lipids uncritically as mimics for the more typical, but less stable ester lipid membranes. Our study addresses specifically the interaction between the antimicrobial peptides novicidin and alamethicin with ether/ester phosphocholine lipid bilayers.

2. MATERIALS AND METHODS

Synthesis, General. Unless otherwise noted, all reactions were carried out under inert atmosphere. Reactions were monitored by thin-layer chromatography (TLC) analysis. Flash chromatography was carried out on Fluka silica gel 60 (230−400 mesh). All solvents and reagents were obtained commercially and were used without further purification with the exception of CH_2Cl_2, which was freshly distilled from CaH_2 prior to use. The products were characterized by ^{1}H (400 MHz) and ^{13}C (100 MHz) NMR spectra. The chemical shifts are reported in ppm relative to solvent residual peak.[19] The following abbreviations are used to indicate multiplicity: s, singlet; d, doublet; dd, double doublet; t, triplet; dt, double triplet; dq, double quartet; m, multiplet. Analytical RP-HPLC was performed using an Agilent 1100 system with a Phenomenex Kinetex column (C18, 4.6 mm i.d. × 150 mm, 2.6 μm, 100 Å) operated at a flow rate of 1 mL/min at 25 °C. Semipreparative RP-HPLC purification was performed on an Agilent 1200 system with a Agilent Zorbax SB column (C18, 9.8 mm i.d. × 250 mm, 5 μm, 300 Å) operated at a flow rate of 5 mL/min at 25 °C. The solvent system was A = 0.1% TFA in H_2O, B = 0.1% TFA in MeCN. Absorbance was monitored at 215 nm, and product percentages are given by peak areas at 215 nm.

Synthesis of H-Aib[$^{15}N,d_6$]-OH. NaCN (5.49 g, 112 mmol) was added to a solution of $^{15}NH_4Cl$ (3.05 g, 56.0 mmol) in H_2O/CH_2Cl_2 1:1 (80 mL) followed by addition of acetone-d_6 (8.24 mL, 112 mmol) and the solution was stirred overnight. The reaction mixture was extracted three times with CH_2Cl_2 and the combined organic phases were dried over $MgSO_4$ and concentrated in vacuo. Thirty milliliters of conc. HCl was added to the resulting residue and the solution was heated at 100 °C for 2 h followed by concentration in vacuo. The resulting colorless residue was suspended in absolute ethanol (75 mL) and filtered. Concentration of the filtrate afforded ^{15}N-α-amino-3,3,3- trideuterio-2-trideuteriomethyl propionic acid (Aib[$^{15}N,d_6$]). (6.2 g, 76%) as a colorless solid. ^{13}C NMR (100 MHz, DMSO-d_6): δ (ppm) 173.3, 55.3 (d, J(^{15}N,^{13}C) = 6.0 Hz), 22.5 (m, 2C).

Synthesis of Fmoc-Aib[$^{15}N,d_6$]-OH. H-Aib[$^{15}N,d_6$]-OH (6.2 g, 56.3 mmol) and Na_2CO_3 (29.8 g, 281 mmol) were dissolved in 200 mL of H_2O and Fmoc-OSu (28.5 g, 84.4 mmol) in 200 mL of dioxane was added, and the resulting suspension was stirred overnight at room temperature. 200 mL of H_2O was added and the resulting mixture was extracted with Et_2O three times. The aqueous layer was acidified with conc. HCl and extracted three times with ethyl acetate. The combined organic phases were dried over $MgSO_4$ and concentrated in vacuo. The crude material was recrystallized from CH_2Cl_2/hexane affording 15.04 g (80%) of Fmoc-Aib[$^{15}N,d_6$]-OH as a colorless solid. ^{1}H NMR (400 MHz, DMSO-d_6): δ (ppm) 12.33 (s, 1H, CO2*H*), 7.76 (d, 2H, J = 7.6 Hz), 7.64 (d, 2H, J = 7.2 Hz), 7.56 (d, 1H, J(^{15}N,^{1}H) = 80 Hz, N*H*), 7.30 (m, 2H), 7.23 (m, 2H), 4.23−4.10 (m, 3H). ^{13}C NMR (100 MHz, DMSO-d_6): δ (ppm) 176.0, 155.1 (d, J(^{15}N,^{13}C) = 26 Hz), 143.9 (2C), 140.8 (2C), 127.7 (2C), 127.1 (2C), 125.3 (2C), 120.1 (2C), 65.4, 55.0 (d, J(^{15}N,^{13}C) = 11 Hz), 46.8, 24.4 (m, 2C). HRMS (ES-TOF): $C_{19}H_{13}D_6{}^{15}NO_4$ [M + Na^+], 355.1559; found, 355.1560.

Synthesis of Fmoc-Aib[$^{15}N,d_6$]-F. Fmoc-Aib[$^{15}N,d_6$]-OH (1.38 g, 4.15 mmol) was dissolved in CH_2Cl_2 (15 mL) and refluxed for 3 h under N_2 with cyanuric fluoride (0.70 mL, 8.30 mmol) and pyridine (0.34 mL, 4.15 mmol). The mixture was extracted two times with ice-cold water (2 × 40 mL), dried over $MgSO_4$, and concentrated in vacuo. The resulting white solid was recrystallized from CH_2Cl_2/hexane, yielding a slightly pink solid (673 mg, 50%). ^{1}H NMR (400 MHz, DMSO-d_6): δ (ppm) 8.16 (d, 1H, J(^{15}N,^{1}H) = 96 Hz, N*H*), 7.89 (d, 2H, J = 7.4 Hz), 7.70 (d, 2H, J = 7.4 Hz), 7.42 (t, 2H, J = 7.4 Hz), 7.33 ((t, 2H, J = 7.4 Hz), 4.38 (d, J = 6.6 Hz, 2H), 4.23 (t, J = 6.6 Hz, 1H). ^{13}C NMR (100 MHz, DMSO-d_6): δ (ppm) 164.5 (d, J = 373.5 Hz), 155.5 (d, J(^{15}N,^{13}C) = 25 Hz), 143.6 (2C), 140.8 (2C), 127.6 (2C), 127.0 (2C), 125.1 (2C), 120.1(2C), 65.8, 54.5 (d, J(^{15}N,^{13}C) = 12 Hz), 46.7, 23.4 (m, 2C). ^{19}F-NMR (377 MHz, DMSO-d_6) δ (ppm) 16.9. HRMS (ES-TOF): $C_{19}H_{13}D_6{}^{15}NO_4$ [M + Na^+], 357.1516; found, 357.1519.

Novicidin. Novicidin was provided by Novozymes A/S. It has the following primary sequence KNLRR IIRKG IHIIK KYF and hence carries 7−8 positive charges at neutral pH.

Alamethicin F30 Aib8[$^{15}N,d_6$]. The peptide, synthesized as reported previously,[20] has the primary sequence Ac-UPUAU AQU*VU GLUPV UUEQ-Phol, where the amino acids are listed in one-letter code with the following abbreviations: Acetyl (Ac), L-Phenylalaninol (Phol), Aib (U), and Aib[$^{15}N,d_6$] (U*). The crude peptide (139 mg) was purified twice by means of semipreparative RP-HPLC using a linear gradient from 50 to 90% B in A over 20 min with a flow rate of 5 mL/min affording 12.2 mg (6%) of the desired product in >95% purity. MALDI-TOF MS: $C_{92}H_{144}D_6N_{21}{}^{15}NO_{25}$ [M + Na^+]; calculated 1993.1, found 1993.0. At neutral pH alamethicin is carrying two positive charges.

Sample Preparation. The bicelles for NMR experiments were made by titrating a stock solution of the various lipids dissolved in chloroform purchased from Avanti Polar Lipids (Alabaster, AL) in amounts such that the molar ratio of the long-chain to short-chain lipids was 3.2 and the total lipid content of the sample was 28% w/v. The long-chain lipids used were 1,2-di-*O*-tetradecyl-*sn*-glycero-3-phosphocholine (14-O-PC) and 1,2-dimyristoyl-*sn*-glycero-3-phosphocholine (DMPC), and the short-chain lipids were 1,2-dihexanoyl-*sn*-glycero-3-phosphocholine (DHPC) or 1,2-di-*O*-hexyl-*sn*-glycero-3-phosphocholine (6-O-PC). The solvent was evaporated from each lipid solution by N_2 flux. Buffer was first added to the long-chain lipids, which upon vortexing formed a homogeneous vesicle suspension, which was added to the dry short-chain lipids. To reduce the viscosity, the lipid suspension was placed over ice bath, and bicelles were formed by vortexing. Finally, the peptide was added to the bicelle solution. The sample tube was cut to proximally 3

cm and was sealed by a rubber plunger as described elsewhere.[14] The total sample volume/peptide to long-chain lipid ratio was 100 μL/1:20 for the alamethicin sample and 200 μL/1:100 for the novicidin sample. All bicelles were mixed in 10 mM phosphate buffer with pH = 6.6. To obtain a 100 μL sample, 28 mg of lipid was used. 1.5 mg of novicidin or 3.6 mg alamethicin was added to the sample.

NMR Experiments. NMR experiments were conducted on a Bruker Avance 400 MHz wide-bore NMR spectrometer employing a Bruker flatcoil triple-resonance probe in double-resonance mode with a homemade solenoidal rf coil accommodating a standard 5 mm NMR tube. The ^{13}C experiment was conducted at 305 K using PISEMA[21] with 20 kHz field strength applied during the SEMA block and decoupling for the DMPC:DHPC sample, and 30 kHz ^{1}H rf field strength for the 14-O-PC:6-O-PC sample. The acquisition time was 25 ms and the interscan delay was 4 s. The Hartmann−Hahn match during cross-polarization employed rf fields of 25 kHz with a 20% ramp on ^{1}H for 3 ms. The ^{15}N spectra were recorded using the SAMPI4[22] pulse sequence utilizing 30 kHz ^{1}H rf field during homonuclear and heteronuclear decoupling. Numerical calculations were performed using in-house prepared custom C programs and scripts for the open source SIMPSON[23] NMR simulation program. The low rf field strength of 20−30 kHz during t_1 is used to avoid sample heating. This proved acceptable as the dynamic averaging in the lipids reduce the homonuclear couplings so much that they can be decoupled with such weak rf fields. Programs and scripts can be found on www.bionmr.chem.au.dk.

CD Spectroscopy. CD spectra were recorded on a Jasco J-810 spectropolarimeter (Jasco Spectroscopic Co., Hachioji City, Japan) with a Jasco PTC-348W1 temperature control unit. Scan speed was set to 100 nm/min, slit width 2 nm. The experiments were carried out in 20 mM Tris−HCl pH 7.5, at 298 K using a 1 mm quartz cuvette from Hellma with a protein concentration of 40 μM. Bicelle solution was added to a final concentration of 2.8% w/v and allowed to equilibrate for at least 1 min before a spectrum was recorded. The samples were measured in three scans and averaged to yield the final spectrum. Background spectra without peptide were subtracted.

3. RESULTS AND DISCUSSION

Phospholipids are the main component of lipid bilayers found in living cells. The integrity of the lipid bilayer is crucial for the function and protection of cells and therefore it is also the target for antimicrobial peptides (AMP). AMPs exercise their antimicrobial effect by altering or puncturing the membrane lipid structure with cell lysis as a result. Several models have been proposed for this lysing effect, including barrel-stave, carpet, and toroidal pore structures (e.g., see reviews[24−27]). Despite numerous studies, the exact mechanisms for the antibiotic activity of most AMPs are still poorly understood and most likely highly diverse in their nature depending on the specific AMP, the membrane composition, and external factors such as hydration, pH, temperature, ion concentration, electrostatic membrane potential, nonprotein/lipid constituents in the membranes, etc. Recent research of the antimicrobial peptides novicidin and pardaxin has, for example, revealed that electrostatics are likely to play a major role in the interaction between lipids and AMPs.[28,29] It is therefore reasonable to assume that the electrostatic nature of the lipids themselves plays an important role in the interaction

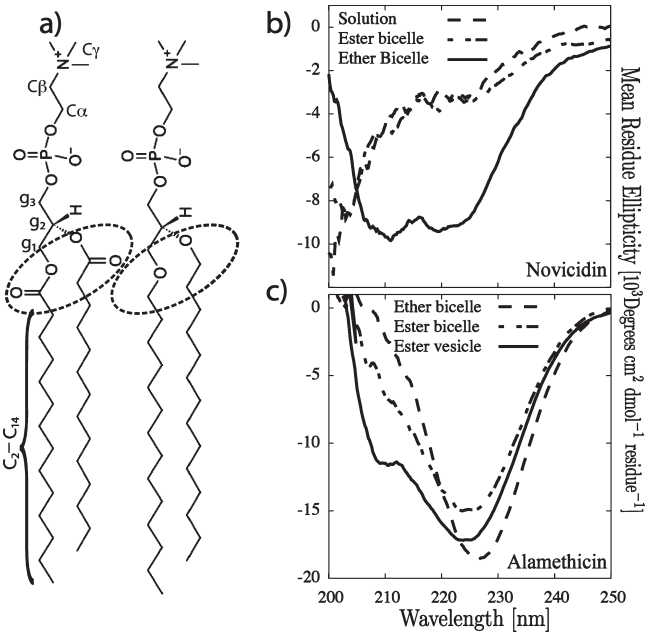

Figure 1. (a) Chemical structure of DMPC (1,2-dimyristoyl-*sn*-glycero-3-phosphocholine) with annotations (left) and 14-O-PC (1,2-di-*O*-tetradecyl-*sn*-glycero-3-phosphocholine) (right). The ether/ester groups are framed by circles. CD spectra of (b) novicidin in solution and in ester and ether bicelles and (c) alamethicin in ester vesicles, and ester and ether bicelles.

process and has to be carefully assessed in the study of AMPs and similar membrane active peptides.

With the aim of studying the interplay between peptide and lipids, we used CD spectroscopy to examine the overall secondary structure of the AMPs in different lipids and oriented solid-state NMR spectroscopy to explore in more detail the conformation, ordering, and dynamics of the peptides in the membranes. Specifically, we used 2D ^{1}H−^{13}C separated-local-field (SLF) NMR on samples with ^{13}C in natural abundance of lipids[30] and ^{1}H−^{15}N SLF (PISEMA[21] or SAMPI4[22]) experiments on ^{15}N-enriched samples for conformational studies at atomic level. For the ^{13}C-based NMR experiments, we titrated the peptide into pure bicelles and looked for spectral changes in 2D PISEMA spectra correlating ^{13}C chemical shifts with ^{1}H−^{13}C dipole couplings as demonstrated previously.[28,29] The observed changes in heteronuclear dipolar couplings relate directly to changes in the order parameter S^2. The order parameter, S_{CH}, defined by eq 1, is a sensitive probe for structural changes of the lipids due to interactions between lipids and peptide.

$$D_{CH} = \left\langle D_{C-H}^{static} \; S_{CH}^{2} \; \frac{3\cos\beta^2 - 1}{2} \right\rangle \qquad (1)$$

with D_{C-H}^{static} = 21.5 kHz, β = 90° for bicelle samples, and D_{CH} representing the sum of the ^{1}H−^{13}C dipole−dipole coupling and J_{CH} the corresponding scalar coupling.

The chemical composition and atom labeling scheme for the lipids used in this study are shown in Figure 1a. The small differences between the lipids have a surprisingly large effect on peptide secondary structure as revealed by the circular dichroism (CD) spectra in Figure 1, b and c, for the AMP novicidin and the peptaibol alamethicin, respectively. Figure 1b shows CD data of novicidin in solution, and in ester and ether bicelles. It is clear that

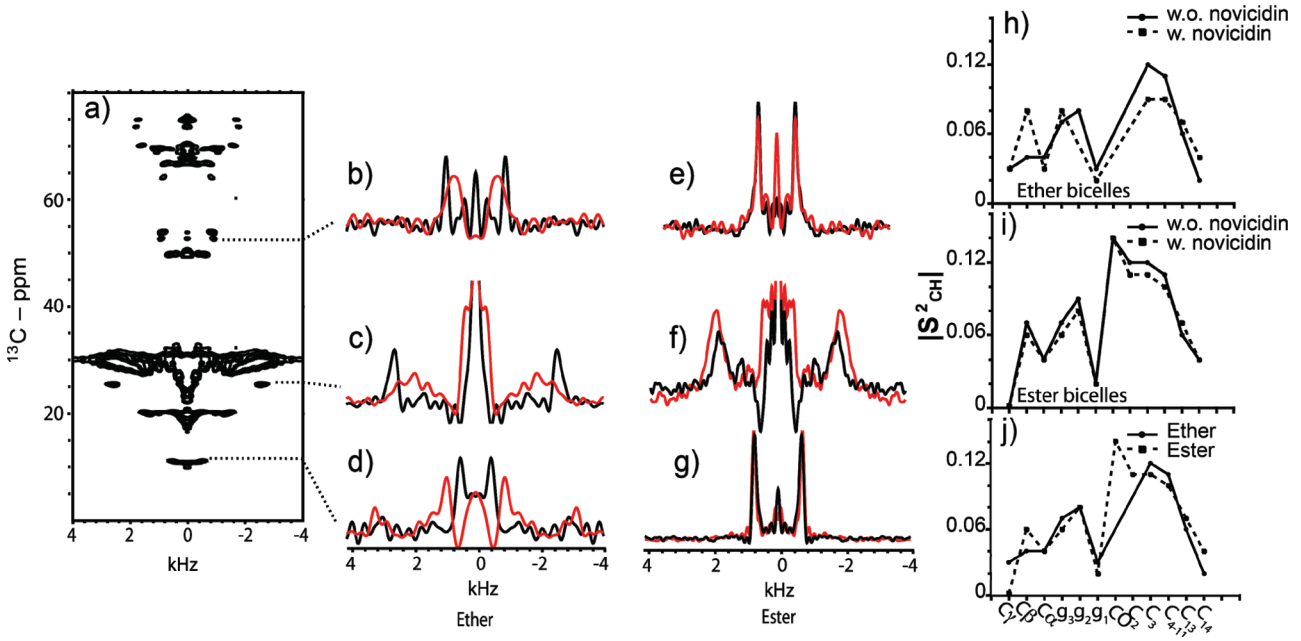

Figure 2. Oriented ^{13}C solid-state NMR of novicidin in ester and ether bicelles. (a) Representative 2D PISEMA spectrum correlating natural abundance ^{13}C chemical shifts (vertical) with ^{1}H−^{13}C dipole−dipole couplings (horizonthal) for a pure ester bicelle. (b−g) ^{1}H−^{13}C dipole−dipole coopling slices taken through the chemical shift of C_α (b,e), C_3 (c,f), and C_{14} (d,g) for ether bicelles (b−d) and ester bicelles (e−g). Black line: without novicidin. Red line: with novicidin in a 1:100 peptide/lipid molar ratio. Assignment of carbon chemical shifts are taken from ref 30. (h−j) Order parameters extracted from ^{13}C natural abundance 2D SLF spectra of ester and ether bicelles with or without novicidin using eq 1 assuming J_{CH} = 150 Hz for all carbons. (h−j) Order parameters for (h) ether bicelles and (i) ester bicelles, in both cases using broken lines to represent lipids with novicidin and solid lines without, while order parameters of pure ester (broken lines) and ether bicelles (full line) are compared in (j).

the peptide does not adopt the same secondary structure in the different environments. Novicidin in buffer and in the DMPC bicelles has a low ellipticity above 210 nm and negative bands around 195 nm indicative of random coiled structure.[31] In 14-O-PC lipids, by contrast, we observe two negative wells around 222 and 208 nm suggesting an α-helical conformation.[32] The CD spectra indicating helical structure in ether bicelles are very similar to the CD spectrum one observes if novicidin interacts with DMPC:DMPG:DHPC bicelles as reported previously.[28] In the same study, calcein release assays revealed that novicidin interacts with zwitterionic lipids and effectively permates the lipid bilayer even though the peptide is considered unstructured. The CD spectra of alamethicin in Figure 1c reveal small differences in the secondary structure of alamethicin in ester and ether bicelles, but more importantly, it is seen that alamethicin does not conform to α-helix in neither of the bicelle systems as is the case for pure DMPC vesicles (Figure 1c, solid line). Overall, from the CD spectra we observe that the cationic AMP novicidin seems to be very sensitive to ether lipids and will fold up in a α-helical-like structure if ether lipids are used while it will remain unstructured if ester lipids are used. Although, to a less degree, alamethicin also seems to be affected structurally when exposed to ether lipids relative to ester lipids, most remarkably, in neither of the systems it adapts the dominant α-helical structures observed in planar DMPC bilayers.[5,33,34]

Figure 2 summarizes the effects on lipid order parameters observed by oriented-sample ^{1}H−^{13}C SLF NMR experiments when novicidin is added to either ether or ester bicelles as compared to the order parameters observed for pure bicelles. Specifically, Figure 2a shows a representative 2D ^{1}H−^{13}C PISEMA spectrum obtained for a pure ester bicelle relying on samples with ^{13}C in natural abundance. Figure 2b−g shows $\omega_1/2\pi$ slices through the chemical shifts of $^{13}C_\alpha$, $^{13}C_3$, and $^{13}C_{14}$ obtained from 2D ^{1}H−^{13}C PISEMA spectra of pure ether/ester bicelles (black lines) and bicelles with novicidin (red lines). Figure 2h−j shows order parameters as calculated by eq 1, with Figure 2h showing those extracted from ether bicelles while Figure 2i shows those from ester bicelles. In both panels, the solid line is order parameters from pure bicelles and the dashed line is with novicidin. Figure 2j compares the order parameters from pure ester and ether bicelles.

It is evident from Figure 2h that the changes in order parameters are more dramatic when novicidin is added to ether bicelles than to the more conventional ester lipids. Especially large changes in order parameters are observed at the C_β, C_3, C_{4-11}, C_{13}, and C_{14} positions. Interestingly, the order parameters for C_{13} and C_{14} *increase* upon addition of novicidin to ether bicelles. This result indicates that novicidin is inserted in a transmembrane manner or at least interacts with the deeply buried C_{13} and C_{14} atoms of the lipid membranes, and that it most likely adapts an α-helical topology in ether bicelles in agreement with the CD spectra in Figure 1b. The observation of an increased order parameter is puzzling at first sight but an explanation could be that if the membrane is filled with bulky novicidin molecules, the rotation of the C_{14} methyl group could be restricted, leading to larger order parameters.

Turning our attention to the ester lipids, Figure 2i shows that virtually no changes in order parameters are observed upon addition of novicidin, which markedly contrasts the situation with ether lipids. The spectral slices in Figure 2e−g display insignificant changes in the line broadening and overall the spectral changes are minute. In particular, no changes are observed for the terminal C_{14} site, indicating that novicidin does not penetrate into the bilayer of DMPC ester lipids in consistency with earlier

dx.doi.org/10.1021/jp110866g |*J. Phys. Chem. B* 2011, 115, 1767–1774

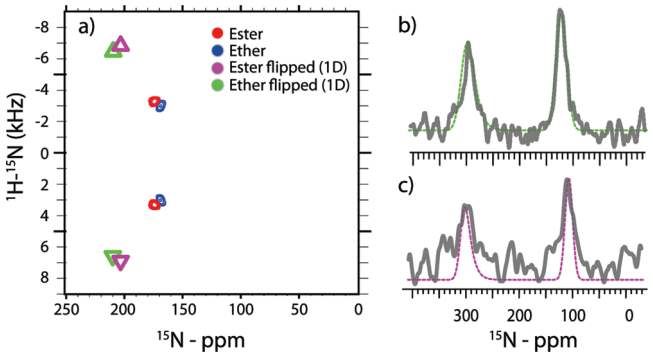

Figure 3. (a) 2D ^{1}H−^{15}N SAMPI4 SLF spectra of d_6-^{15}N-Aib$_8$-labeled alamethicin in ester (red contours) and ether (blue contours) bicelles in standard nonflipped orientation (bicelle normal perpendicular to the $\mathbf{B}_0$ field). (b,c) 1D homonuclear FSLG-decoupled spectra showing chemical shift and dipole−dipole coupling patterns for alamethicin in (b) ether and (c) ester bicelles flipped by lanthanides (bicelle normal parallel to $\mathbf{B}_0$) along with simulated spectra. All spectra reference values and spectral widths have been scaled as described in the text so that all spectra can be directly compared. The colored triangles in (a) refer to the spectral parameters extracted from (b) and (c). The difference in S/N between spectra b and c is due to different number of scans: (b) represents 30 000 scans while (c) represents only 10 000 scans.

observations.[28,35] The NMR data clearly demonstrate that novicidin interacts with ester and ether membranes in different ways. We note that the CD spectra (Figure 1) formally agree well with the solid-state NMR data and support that novicidin interacts quite differently with the two lipid types.

Having shown the effects ether lipids have on the AMP novicidin, we turn to another well-studied AMP alamethicin. Alamethicin also proves to behave differently in ether bicelles as compared to ester bicelles, and furthermore it turns out to interact in an unexpected manner with lipid bicelles. Numerous papers have reported studies of singly or sparsely ^{15}N- or ^{2}H-labeled alamethicin molecules in mechanically oriented DMPC bilayers,[5,33] DOPC bilayers,[36] DMPC vesicles,[20] short-chain ether (DHPC), and ester lipids (DPPC or POPC),[37] and in isotropic DMPC:DHPC bicelles.[34] All these studies point toward a transmembrane helical model for alamethicin in lipid bilayers at high peptide:lipid ratios. In addition, alamethicin has been studied in anionic membranes consisting of POPE/POPG 3:1 lipids, where alamethicin adopted an in-plane orientation.[37] Besides, unlabeled alamethicin has been studied in the presence of ether lipids by oriented solid-state ^{31}P NMR spectroscopy.[17]

To explore the membrane-bound conformation of alamethicin, Figure 3 shows an overlaid set of 2D ^{1}H−^{15}N SAMPI4 SLF[22] spectra and 1D FSLG homonuclear decoupled spectra recorded for alamethicin-Aib8[^{15}N,d_6] in differently oriented (flipped by lanthanides[38] or unflipped) ester and ether lipids. The spectra in Figure 3 have been adjusted according to the order parameter measured from ^{31}P spectra of the same samples shown in Figure 4. Spectral width and reference point were adjusted according to the formulas $SW_{new} = SW \times sf$ and $REF_{new} = REF + (REF\text{-}ISO) \times (sf\text{-}1)$, where the scaling factor sf is taken as the ratio of the $\sigma_{||}$ element of the ^{31}P tensor in a hydrated bilayer and the resonance frequency of the aligned phosphorus spectra (31 ppm), SW is the spectral width, REF is the spectrum reference frequency, and ISO is the isotropic chemical shift of 126 ppm. In this manner, all the spectra from bicelles of either orientation can be directly compared to unravel spectral differences for peptides incorporated into ester or ether bilayers.

As the peptide only contains one ^{15}N label, which only provides information about the orientation of the peptide plane in which the label is residing[39] but can be interpreted in terms of alignment of full helices provided the label is present inside a helical segment, we interpret the 2D spectra in combination with the CD spectra in Figure 1c. As addressed above, the CD spectra reveal only small differences in the secondary structure of alamethicin in ester and ether bicelles but more remarkably that alamethicin is not represented by an α-helix in neither of the bicelle systems as is seen for the DMPC vesicles (Figure 1c, solid line). This may explain why we observe order-parameter-corrected ^{15}N chemical shifts around 160 ppm and dipole−dipole couplings in the order of 2−3 kHz for alamethicin in nonflipped bicelles. In contrast, if we flip the bicelles by addition of Yb^{3+} ions (5 mM), we observe order-parameter-corrected ^{15}N chemical shifts around 210 ppm and dipolar couplings in order of 6−7 kHz which compare well with an transmembrane helix and with what we have observed in mechanical oriented bilayers.[5,33]

The difference between the chemical shift and dipole−dipole coupling data observed for alamethicin in bicelles oriented with the bilayer normal perpendicular and parallel with the magnetic field suggests that the peptide−lipid anchoring is very loose since it is altered by the addition of Yb^{3+}, e.g., through the lanthanide-induced change in magnetic susceptibility. We note that similar observations were recently reported in a study by Ouellet et al.[40] At the same time, we note that the ^{15}N data obtained for alamethicin in flipped bilayers compare favorably with previous studies of alamethicin in oriented lipid bilayers. The same is true for the ^{2}H quadrupole couplings of Aib8-d_6 labeled alamethicin, which we previously have reported to be 6.7 and 10.0 kHz for the two methyl groups, respectively.[20] Figure 4 shows 1D ^{2}H and FSLG homonuclear decoupled ^{15}N spectra of flipped ether bicelles. In the deuterium spectrum, we observe two overlapping splittings at around 9.4 kHz at 311 K (Figure 4a), and 8.4 kHz at 318 K (Figure 4d). Although the current values for the quadrupole coupling are similar to those previously reported, none of the current ^{2}H spectra can positively confirm or dismiss the presence two distinct resonances. This and the slight difference in the observed quadrupole couplings suggest that the residue-specific structure and dynamics are somewhat different in mechanically oriented ester bilayers and magnetically oriented ether bicelles.

Addressing the ^{31}P spectra, it is evident that both types of lipids in the case of nonoriented pure vesicles give rise to similar ^{31}P powder spectra dominated by the chemical shift anisotropy (black lines in Figure 4, c and f). For bicelles oriented in the normal fashion with the bilayer normal perpendicular to the magnetic field, the ^{31}P spectrum displays a dominant peak at −12 ppm and a smaller peak at −6 ppm, which are typically assigned to the long- and short-chain lipid headgroups, respectively. We note that, for bicelles flipped using lanthanide ions, the peaks broaden because of the paramagnetic lanthanide ions. In both cases dominant peaks for the long- and short-chain lipids indicate a good but not perfect alignment with least ordering for the ether bicelles. The small peak at 0 ppm is due to the 10 mM phosphate buffer and possibly minor amounts of small isotropic micelles. The ^{15}N spectra obtained for the flipped bilayers formed by ether lipids using homonuclear (FSLG) proton decoupling display dominant peaks corresponding to a ^{1}H−^{15}N dipole−dipole coupling constant of 6.4 kHz and a ^{15}N chemical shift of 212 ppm, being

dx.doi.org/10.1021/jp110866g |J. Phys. Chem. B 2011, 115, 1767–1774

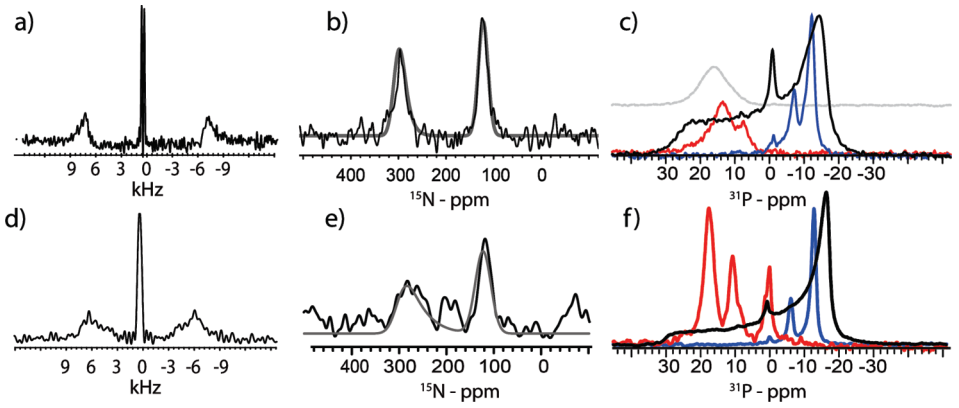

Figure 4. One-dimensional oriented-sample ^{2}H, ^{15}N, and ^{31}P spectra of alamethicin in ether and ester lipids. ^{2}H (a,d) and FSLG-decoupled ^{15}N (b,e) spectra of d_6-^{15}N-Aib$_8$-labeled alamethicin in flipped ether bicelles collected at 311 K (a,b) and 318 K (d,e). (c) ^{31}P spectra of ether lipid vesicles (black), nonflipped bicelles (blue), and flipped bicelles at 311 K; the gray spectrum is flipped bicelles at 318 K. (f) ^{31}P spectra of ester lipid bicelles and vesicles (black), unflipped bicelles (blue), and flipped bicelles at 311 K (red). The ^{2}H and FSLG decoupled ^{15}N spectra are scaled/referenced according to observed order parameters (see text).

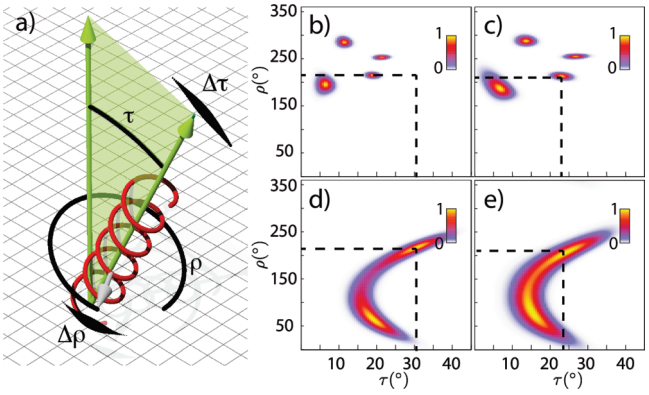

Figure 5. (a) Definition of the helix-orientation angles τ,ρ and the fluctuations $\Delta\tau$ and $\Delta\rho$. The tilt angle τ is defined as the angle between the membrane normal and the helix axis. The pitch angle, ρ, is defined relative to the plane spanned by the membrane normal vector and the helix axis. (b,d) Restriction plots[20] compatible with the spectral data presented in Figure 4d,e, assuming static anchoring of alamethicin in the ester lipids, i.e., no dynamics. Notice that the ^{15}N data (d) and ^{2}H data (b) do not agree on a common conformation (i.e., set of orientational angles). (c,e) Restriction plots of the spectral data presented in Figure 4d,e assuming a dynamic anchoring with Gaussian distributed fluctuations of rotational pitch (ρ) and peptide tilt angle (τ) with half-width at half-height of 36° and 20° for the Gaussian profiles, respectively. Notice how the data agree on the same structure.

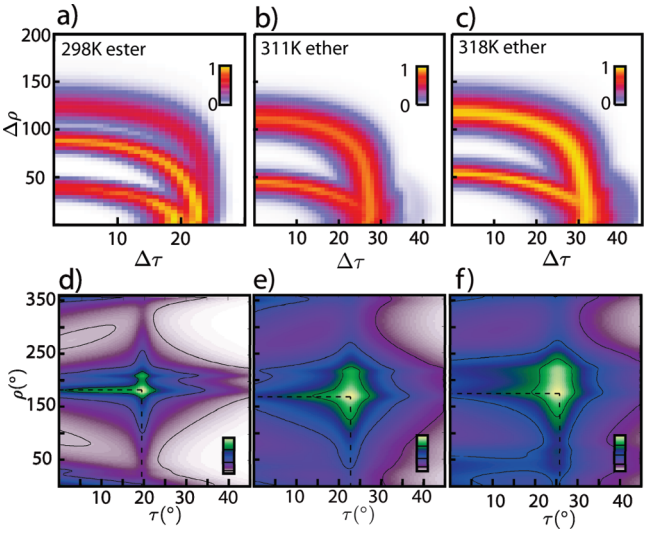

Figure 6. Dynamic anchoring of alamethicin in ester and ether bilayers at different temperatures. Multiple combinations of $\Delta\tau$, $\Delta\rho$ will give rise to overlap of ^{15}N- and ^{2}H-based restriction plots. (a) Maximum of the product (normalized to 1; see color bar) between ^{15}N and ^{2}H restriction plots assuming different amplitudes for $\Delta\tau$ and $\Delta\rho$. (b) The same as in (a) but for alamethicin in ether bicelles at 311 K while (c) is for 318 K. (d−f) So-called conformational probability plots[41] which are a summation of products between ^{15}N and ^{2}H data restriction plots folded with the corresponding Gaussian distribution to reflect the probability of a given conformation in (d) ester lipids at 298 K, (e) ether lipids at 311 K, and (f) ether lipids at 318 K.

indicative of a transmembrane conformation. The normal ^{1}H decoupled 1D spectra (not shown), and in particular the FSLG decoupled spectra, where the observed differential line broadening of the two peaks is indicative of static orientational disorder,[33] clearly indicate a lower degree of alignment (larger mosaic spread) and a higher degree of segmental motion (vide infra) than observed for the corresponding ester lipids.

Following the approach to determine residue-specific information on the membrane anchored dynamics of alamethicin,[41] we can make a dynamic model of alamethicin in lipid bicelles compatible with the observed NMR spectra in Figure 4 and compare with the dynamics observed in mechanical oriented bilayers. The outline of the analysis is shown in Figure 5, while the results are given in Figure 6. The model is based on the availability of multiple orientational constraints on a single residue, which allows us to expand on the structural model, which NMR data can describe. With four independent measurements on a single residue, it is possible not only to uniquely determine the orientation in terms of tilt (τ) and pitch (ρ) angles (see definitions of angles in Figure 5a)[9] but also determine the fluctuations of the peptide in the membrane on a fast time scale of these parameters ($\Delta\tau$ and $\Delta\rho$). These numerical calculations were performed using custom C programs and SIMPSON[23] scripts. The experimental parameters used for the analysis are given in Table 1.

Table 1. Experimental Parameters Used for Calculation of the Restriction Plots Presented in Fig 5'[a]

	298 K (ester vesicle and oriented bilayer)	311 K (ether bicelle)	318 K (ether bicelle)
^{15}N chemical shift (ppm)	214 ± 2	212 ± 12	204 ± 12
^{1}H−^{15}N dipole−dipole coupling (Hz)	7114 ± 500	6400 ± 400	6800 ± 500
^{2}H quadrupolar coupling (kHz)	6.7 ± 1.5, 10.1 ± 1.5	9.42 ± 3	8.3 ±3

[a] From micelle-reconstituted alamethicin, we were able to measure the orientation-dependent quadrupolar coupling for each individual methyl group.[20] The quadrupolar couplings for each methyl group are overlapping for the bicelles samples used in this study and hence only one coupling is reported. Parameters for the nuclear spin interactions can be found in ref 20.

The restriction plots in Figure 5 report peptide orientations compatible with the ^{2}H (b,c) and ^{15}N (d,e) data at 311 K assuming a static anchoring of alamethicin in the lipid bilayer, Figure 5b,d. The discrepancies between the ^{2}H and ^{15}N data underline the defectiveness of the static-anchoring model. If one instead assumes dynamics in the anchoring of the peptide in the lipid bilayer, Figure 5c,e, the observed spectral characteristics can be explained by a conformational dependent scaling factor, $\overline{\kappa_\lambda}(\rho,\tau,\Delta\rho,\Delta,\tau)$, in eq 2,[41] which for a given nuclear spin interaction λ (e.g., ^{15}N chemical shift, ^{2}H quadrupolar coupling, and ^{1}H−^{15}N dipole−dipole coupling) represents a Gaussian distribution of conformations described by a conformational scaling factor, $\kappa_\lambda(\rho,\tau)$, and a half-width at half-height (hwhh) spread of $(\Delta\rho,\Delta\tau)$. This distribution fits a model of a membrane-anchored helix, which fluctuates in tilt $(\Delta\tau)$ and pitch $(\Delta\rho)$ angles according to the definitions in Figure 5a.

$$\overline{\kappa_\lambda}(\rho,\ \tau,\ \Delta\rho,\ \Delta\tau) = \frac{\ln 2}{\pi\Delta\rho\Delta\tau}\int_{-\infty}^{\infty}\int_{-\infty}^{\infty}\kappa_\lambda(\rho+r,\ \tau+t)\ \exp\left[-\ln 2\left(\left(\frac{r}{\Delta\rho}\right)^2+\left(\frac{t}{\Delta\tau}\right)^2\right)\right]\mathrm{d}r\ \mathrm{d}t \qquad (2)$$

Figure 5c,e shows restriction plots based on a model where $\Delta\tau$ = 20° and $\Delta\rho$ = 36°. Notice that, under such circumstances, the data are compatible with a somewhat different conformation than suggested by the static model, but more importantly *both* the ^{15}N and ^{2}H data now agree on the same conformation as indicated by the dotted lines. This is a clear-cut example where we, in order to describe the observed NMR data, need to take into account the dynamics of the membrane anchoring.

Not only the initially assumed values $\Delta\tau$ = 20° and $\Delta\rho$ = 36° are in agreement with the experimental data. In fact, a continuum of solutions exists as outlined by the plots in Figure 6. Using the approach outlined above, Figure 6a−c reports the maximum value (i.e., the best agreement with experimental data) in products of restriction plots from ^{2}H and ^{15}N data at different $\Delta\tau$ and $\Delta\rho$ values. For the ether sample at 311 K (Figure 6b), the values $\Delta\tau$ = 20° and $\Delta\rho$ = 36° indeed fall on the yellow trace. Figure 6d−f presents a sum of all the multiplied restriction plots registered to have high agreement with experimental data giving rise to the yellow ridges in Figure 6a−c, each convoluted by the Gaussian function corresponding to their $\Delta\tau$ and $\Delta\rho$ values, and finally normalized to a total probability of 1. Such plots are referred to as conformation probability plots, as they will represent the probability of finding the helix segment in a certain conformation according to our Gaussian model based on the ^{1}H−^{15}N and ^{2}H solid-state NMR data.[41] Parts a and d of Figure 6 are identical to those previously presented[41] and summarize the same analysis for alamethicin in macroscopically oriented ester bilayers at 298 K. The conformation probability plots in Figure 6b,e indicate that alamethicin is considerably more loosely anchored in ether membranes than in ester membranes.

The looser anchoring in the ether membranes may partly be ascribed to the higher temperature (311 K) used for the ether membranes relative to the ester membrane (298 K). 311 K is the lowest temperature allowing oriented ether bicelles. This is reinforced by the observation that, at even higher temperatures, the dynamic fluctuations are even larger as is seen in Figure 6c,f, which are based on data collected at 318 K. Membrane-thinning effects observed when heating membranes could explain the slightly larger average tilt angle observed at 318 K.[42] In order for alamethicin to achieve optimum hydrophobic match, larger tilt angles are expected. Simple geometric consideration suggests that the membrane should be thinned by roughly 0.9 Å, if the total bilayer thickness is 30 Å, in order to account for the increase in tilt angles of approximately 4°. This is more than expected from other studies of membrane thinning due to temperature rising which is 0.35 Å assuming a decrease in thickness of −0.05 Å/K.[43] According to such a model the alamethicin tilt angle should increase from 22° to 24° as a consequence of a temperature increase from 311 to 318 K. But as can be seen from the ^{31}P spectrum of the bicelle at 318 K, one is no longer able to distinguish between rim and bilayer since the spectrum appears just as one featureless broad peak. This suggests that 6-O-PC and 14-O-PC are mixed together which would give a highly unordered bilayer that would be noticeably thinner because of the high population of 6-O-PC mixed with 14-O-PC in the bilayer. In conclusion, we observe looser anchoring of alamethicin in ether bicelles compared to ester bilayers. This may be due to the higher temperatures needed in order to obtain alignment of bicelles. As of now, the observation that the orientation of the bicelle apparently influences on the peptide conformation is the subject of further investigation.

4. CONCLUSION

In conclusion, we have experimentally demonstrated adverse effects of the lipid environments on the structure and conformation of membrane-associated peptides. This reinforces, in general terms, the need for careful attention to the full system (protein and environment) in structural studies of membrane proteins, here with primary focus on small antimicrobial peptides. In the context of increasingly used solid-state NMR procedures, it reinforces that ether lipids are not always a suitable replacement for ester lipids when studying interaction between peptides and lipid bilayers. We have observed that especially the fold and possibly the oligomerization of AMPs may be severely altered if ether lipids are used instead of the natural occurring ester lipids. Especially, the secondary structure of novicidin is markedly different in ester compared to ether bicelles. We have also observed the impact of the rigidity of the anchoring of alamethicin in the

membrane and observed how the higher temperatures needed for aligning bicelles induce increased dynamic fluctuations of the peptide and induce shifts in average tilt angles possibly because of membrane thinning due to high temperatures. We anticipate that these effects will affect many other small AMPs that exercise their antibiotic effect through intricate interactions with the lipid bilayer. Hence, in addition to the biophysical relevance of the action of AMPs in different lipid systems, we here state that the greatest care should be taken when using ether lipids instead of ester when investigating AMPs. Interestingly, our results also indicate that care should be taken when using bicelles as alternatives to more rigid planar bilayers in studies of AMPs, as evidenced here by the observation that alamethicin does not conform to a true α-helix in either unflipped ester or ether bicelles and accordingly appears inconsistent with data from previous oriented solid-state NMR studies of alamethicin in mechanically oriented DMPC bilayers and lipid vesicles.

AUTHOR INFORMATION

Corresponding Author

*E-mail: ncn@inano.dk (N.C.N.); tv@chem.au.dk (T.V.).

ACKNOWLEDGMENT

We acknowledge support from the Danish National Research Foundation and Lundbeckfonden. S.K.H. acknowledges support by a grant from Novo Nordisk Fonden. Drs. Hans Henrik Kristensen and Per Holse Mygind, Novozymes A/S, are acknowledged for their generous donations of novicidin used in this study.

REFERENCES

(1) Bechinger, B.; Kim, Y.; Chirlian, L. E.; Gesell, J.; Neumann, J. M.; Montal, M.; Tomich, J.; Zasloff, M.; Opella, S. J. *J. Biomol. NMR* **1991**, *1*, 167.

(2) Opella, S. J.; Marassi, F. M.; Gesell, J. J.; Valente, A. P.; Kim, Y.; Oblatt-Montal, M.; Montal, M. *Nat. Struct. Biol.* **1999**, *6*, 374.

(3) Marassi, F. M.; Ma, C.; Gesell, J. J.; Opella, S. J. *J. Magn. Reson.* **2000**, *144*, 156.

(4) Wang, J.; Denny, J.; Tian, C.; Kim, S.; Mo, Y.; Kovacs, F.; Song, Z.; Nishimura, K.; Gan, Z.; Fu, R.; Quine, J. R.; Cross, T. A. *J. Magn. Reson.* **2000**, *144*, 162.

(5) Bak, M.; Bywater, R. P.; Hohwy, M.; Thomsen, J. K.; Adelhorst, K.; Jakobsen, H. J.; Sorensen, O. W.; Nielsen, N. C. *Biophys. J.* **2001**, *81*, 1684.

(6) Vosegaard, T.; Kamihira-Ishijima, M.; Watts, A.; Nielsen, N. C. *Biophys. J.* **2008**, *94*, 241.

(7) Ketchem, R. R.; Hu, W.; Cross, T. A. *Science* **1993**, *261*, 1457.

(8) Cross, T. A.; Opella, S. J. *Curr. Opin. Struct. Biol.* **1994**, *4*, 574.

(9) Bechinger, B.; Gierasch, L. M.; Montal, M.; Zasloff, M.; Opella, S. J. *Solid State Nucl. Magn. Reson.* **1996**, *7*, 185.

(10) Sanders, C. R.; Prestegard, J. H. *Biophys. J.* **1990**, *58*, 447.

(11) Sanders, C. R.; Schwonek, J. P. *Biochemistry* **1992**, *31*, 8898.

(12) Howard, K. P.; Opella, S. J. *J. Magn. Reson. B* **1996**, *112*, 91.

(13) Aussenac, F.; Lavigne, B.; Dufourc, E. J. *Langmuir* **2005**, *21*, 7129.

(14) De Angelis, A. A.; Opella, S. J. *Nat. Protoc.* **2007**, *2*, 2332.

(15) Ruocco, M. J.; Siminovitch, D. J.; Griffin, R. G. *Biochemistry* **1985**, *24*, 2406.

(16) Persson, S.; Killian, J. A.; Lindblom, G. *Biophys. J.* **1998**, *75*, 1365.

(17) Dave, P. C.; Billington, E.; Pan, Y. L.; Straus, S. K. *Biophys. J.* **2005**, *89*, 2434.

(18) Paltauf, F. *Chem. Phys. Lipids* **1994**, *74*, 101.

(19) Gottlieb, H. E.; Kotlyar, V.; Nudelman, A. *J. Org. Chem.* **1997**, *62*, 7512.

(20) Bertelsen, K.; Pedersen, J. M.; Rasmussen, B. S.; Skrydstrup, T.; Nielsen, N. C.; Vosegaard, T. *J. Am. Chem. Soc.* **2007**, *129*, 14717.

(21) Wu, C. H.; Ramamoorthy, A.; Opella, S. J. *J. Magn. Reson. A* **1994**, *109*, 270.

(22) Nevzorov, A. A.; Opella, S. J. *J. Magn. Reson.* **2007**, *185*, 59.

(23) Bak, M.; Rasmussen, J. T.; Nielsen, N. C. *J. Magn. Reson.* **2000**, *147*, 296.

(24) Bechinger, B. *Biochim. Biophys. Acta* **1999**, *1462*, 157.

(25) Zasloff, M. *Nature* **2002**, *415*, 389.

(26) Brogden, K. A. *Nat. Rev. Microbiol.* **2005**, *3*, 238.

(27) Hale, J. D.; Hancock, R. E. *Expert Rev. Anti-Infect. Ther.* **2007**, *5*, 951.

(28) Vad, B.; Thomsen, L. A.; Bertelsen, K.; Franzmann, M.; Pedersen, J. M.; Nielsen, S. B.; Vosegaard, T.; Valnickova, Z.; Skrydstrup, T.; Enghild, J. J.; Wimmer, R.; Nielsen, N. C.; Otzen, D. E. *Biochim. Biophys. Acta., Proteins Proteomics* **2010**, *1804*, 806.

(29) Vad, B. S.; Bertelsen, K.; Johansen, C. H.; Pedersen, J. M.; Skrydstrup, T.; Nielsen, N. C.; Otzen, D. E. *Biophys. J.* **2010**, *98*, 576.

(30) Dvinskikh, S.; Dürr, U.; Yamamoto, K.; Ramamoorthy, A. *J. Am. Chem. Soc.* **2006**, *128*, 6326.

(31) Venyaminov, S.; Vassilenko, K. S. *Anal. Biochem.* **1994**, *222*, 176.

(32) Holzwarth, G.; Doty, P. *J. Am. Chem. Soc.* **1965**, *87*, 218.

(33) Vosegaard, T.; Bertelsen, K.; Pedersen, J. M.; Thogersen, L.; Schiott, B.; Tajkhorshid, E.; Skrydstrup, T.; Nielsen, N. C. *J. Am. Chem. Soc.* **2008**, *130*, 5028.

(34) Dittmer, J.; Thogersen, L.; Underhaug, J.; Bertelsen, K.; Vosegaard, T.; Pedersen, J. M.; Schiott, B.; Tajkhorshid, E.; Skrydstrup, T.; Nielsen, N. C. *J. Phys. Chem. B* **2009**, *113*, 6928.

(35) J. Dorosz, S. K., Y.; Gofman, D. E.; Otzen, N.; Ben-Tal, N. C.; Nielsen; Jelinek, R. *J. Phys. Chem. B* **2010**, *114*, 11053.

(36) Salnikov, E. S.; Friedrich, H.; Li, X.; Bertani, P.; Reissmann, S.; Hertweck, C.; O'Neil, J. D. J.; Raap, J.; Bechinger, B. *Biophys. J.* **2009**, *96*, 86.

(37) Salnikov, E.; Aisenbrey, C.; Vidovic, V.; Bechinger, B. *Biochim. Biophys. Acta* **2010**, *1798*, 258.

(38) Prosser, R. S.; Hwang, J. S.; Vold, R. R. *Biophys. J.* **1998**, *74*, 2405.

(39) Bechinger, B.; Sizun, C. *Concepts Magn. Reson., Part A* **2003**, *18A*, 130.

(40) Ouellet, M.; Voyer, N.; Auger, M. *Biochim. Biophys. Acta* **2010**, *1798*, 235.

(41) Bertelsen, K.; Paaske, B.; Thogersen, L.; Tajkhorshid, E.; Schiott, B.; Skrydstrup, T.; Nielsen, N. C.; Vosegaard, T. *J. Am. Chem. Soc.* **2009**, *131*, 18335.

(42) Nagle, J. F.; Tristram-Nagle, S. *Curr. Opin. Struct. Biol.* **2000**, *10*, 474.

(43) Pan, J.; Tristram-Nagle, S.; Kucerka, N.; Nagle, J. F. *Biophys. J.* **2008**, *94*, 117.